

Topography of phase diagrams in binary fluid mixtures: A mean-field lattice density functional study

Dirk Woywod* and Martin Schoen†

Stranski-Laboratorium für Physikalische und Theoretische Chemie, Sekr. C 7, Fakultät für Mathematik und Naturwissenschaften, Technische Universität Berlin, Straße des 17. Juni 135, D-10623 Berlin, Germany

(Received 3 September 2005; published 12 January 2006)

We employ mean-field lattice density functional theory to calculate complete phase diagrams of binary fluid mixtures composed of molecules of equal size. We consider asymmetric binary mixtures in which the attraction strength between like molecules of either species differs as well as the attractivity between a pair of unlike molecules. Focusing on the topology of phase diagrams in the space spanned by the thermodynamic fields temperature T , (mean) chemical potential $\mu \equiv (\mu_A + \mu_B)/2$, and incremental chemical potential $\Delta\mu \equiv (\mu_A - \mu_B)/2$ (μ_A , μ_B are chemical potentials of pure mixture components A and B, respectively), we present an argument which precludes the existence of tricritical points (TCPs) in binary mixtures in *general*. This is a consequence of a purely geometrical argument based upon an analysis of the number of ways in which coexistence surfaces can be joined in the (Euclidian) space of T , μ , and $\Delta\mu$. However, we show that by the same token, TCPs may exist in cases where the mixture possesses some special symmetry. These latter results are in qualitative agreement with earlier works where, however, only special cuts through the complete phase diagrams were considered so that the important relation between existence of TCPs and symmetry properties of the mixture cannot be fully appreciated.

DOI: [10.1103/PhysRevE.73.011201](https://doi.org/10.1103/PhysRevE.73.011201)

PACS number(s): 61.20.Ja, 61.30.Hn, 68.15.+e, 68.60.-p

I. INTRODUCTION

If one is dealing with fluids (i.e., gases or liquids) one is almost always confronted with mixtures composed of two or more components. Because of the interaction between molecules of the different components, mixtures exhibit a much richer phase behavior than either one of the pure components of which they consist. For example, such mixtures may phase separate not only into a gaseous and a single liquid phase but into a mixed as well as several demixed liquid phases in which one of the components is the dominating one. An understanding of the relation between the rather complex phase behavior of fluid mixtures on one hand and the interaction between its various molecular constituents is, therefore, of vital interest both from a fundamental [1] and a technological point of view (see, for example, Ref. [2]). In this latter case, one is frequently facing the problem that a mixture needs to be separated into its pure components [3].

Specializing immediately to the simplest mixture, namely the binary one composed of just two components A and B, say, it is, therefore, not surprising that quite a bit of work was invested over the past 30 years or so to elucidate the various aspects of its phase behavior. For example, in their pioneering work, van Konynenberg and Scott demonstrated the complexity of this phase behavior for a binary van der Waals mixture [4]. In agreement with Furman and Griffiths [5,6], van Konynenburg and Scott introduced five principal classes of phase diagrams depending on the relative sizes of the

molecules and the strengths of their intermolecular interactions (see Ref. [1] for a review). Several other authors like Boshkov [7] (Ree equation), Meijer *et al.* [8,9] (lattice fluid), Deiters *et al.* [10,11] (Redlich-Kwong and Carnahan-Starling-Redlich-Kwong equation), van Pelt and de Loos [12] (simplified perturbed hard chain theory) have verified and extended this classification scheme by introducing, for example, a sixth principal class for dipolar mixtures together with a number of subclasses.

However, all these previous works focused only on special cuts through the phase diagram (such as critical lines or triple lines along which one has three-phase coexistence) rather than considering *complete* (i.e., three-dimensional) phase diagrams in the space spanned by the three thermodynamic fields necessary to uniquely specify the thermodynamic state of a binary mixture. This is because the construction of such a complete phase diagram requires access to the relevant thermodynamic potential which is difficult if one determines the phase behavior solely from semiempirical equations of state as in the earlier works [4,7,10,11] (see above). In more recent years, more microscopically motivated studies aimed at a more comprehensive picture of this phase behavior [13–27] by employing methods such as density functional theory [14], integral equations [25,26], hierarchical reference theory [28], molecular dynamics [27], or Monte Carlo computer simulations [15–18,24]. However, because of the much greater computational effort required in particular by these latter groups of studies, they were all limited to rather narrow ranges of model or thermodynamic parameters. For example, in most cases, special mixing rules were employed by which the interaction strength between a pair of unlike molecules is calculated from the ones between either pair of like molecules. In addition, the focus is often on symmetric mixtures in which the interaction between like

*Electronic address: dirk.woywod@fluids.tu-berlin.de†Electronic address: martin.schoen@fluids.tu-berlin.de

molecules of either species is taken to be the same as well as the chemical potentials of both components.

However, as we shall demonstrate here, knowledge of the complete (three-dimensional) phase diagram is essential not only to classify the mixture type properly but more importantly to understand the existence of so-called tricritical points (TCPs) in binary fluid mixtures. A TCP is a point in thermodynamic state space where three coexisting fluid phases become critical simultaneously. TCPs have been reported in the literature many times before regardless of the specific approach or model taken (see, for example, Ref. [4]).

However, based upon simple geometrical considerations, we argue that in a *general* binary fluid mixture, TCPs must not exist. Applying these geometrical arguments to the complete phase diagrams, we also show that TCPs might very well exist if the mixture possesses a certain symmetry. In this latter case, our results are in (qualitative) agreement with all previous studies where, however, no explanation for the existence of TCPs is given. Moreover, these previous studies do not recognize the important relation between the topology of the phase diagram and the existence of TCPs. An analysis of this relation is one of the focal points of the present study following in spirit the geometrical approach to equilibrium thermodynamics presented in Ref. [29].

The remainder of our paper is organized as follows. In Sec. II A, we introduce our model. In particular, we discuss three limiting cases of the thermodynamic fields where the mixture degenerates to an *effective* pure fluid. In Sec. III, we review briefly the classification scheme of van Konynenburg and Scott [4]. Moreover, we present phase diagrams for symmetric as well as for asymmetric mixtures and analyze their topology. Finally, in Sec. IV, we discuss our findings in the context of earlier studies and summarize the geometrical concept linking the topology of complete phase diagrams to the existence of TCPs in binary fluid mixtures.

II. THEORETICAL CONSIDERATIONS

A. Model system

We consider a binary fluid (gaseous or liquid) mixture consisting of N_A molecules of species A and N_B molecules of species B. The molecules of both species are assumed to be equal in size differing only in the attraction strengths ϵ_{AA} , ϵ_{AB} , and ϵ_{BB} of an A-A, A-B, and B-B pair of molecules, respectively. The mixture is contained in some volume V , where we immediately simplify the subsequent analysis by assuming that V can be discretized according to a regular lattice of \mathcal{N} cubic cells such that $V = \mathcal{N}\ell^3$, where ℓ is the lattice constant. To specify individual arrangements of molecules (i.e., configurations) on that lattice, we introduce the occupation-number vector $S \equiv (s_1, s_2, \dots, s_{\mathcal{N}})$, where the occupation number is a triple-valued integer, namely,

$$s_k = \begin{cases} +1 & \text{cell occupied by molecule of species A} \\ 0 & \text{empty cell} \\ -1 & \text{cell occupied by molecule of species B,} \end{cases} \quad k = 1, \dots, \mathcal{N}. \quad (2.1)$$

We assume pairwise additivity of all interactions which we

model according to square-well potentials and take the width of the attractive well (of depth $\epsilon_{ij} \geq 0$, $i, j = A, B$) to be equal to ℓ . Hence, each cell may be occupied by one molecule at most and only nearest neighbors on the lattice attract each other.

The Hamiltonian governing the evolution of our model in state space may then be cast as [22]

$$\mathcal{H}(S) = -\epsilon_{AA}N_{AA}(S) - \epsilon_{AB}N_{AB}(S) - \epsilon_{BB}N_{BB}(S) - \mu_A N_A(S) - \mu_B N_B(S), \quad (2.2)$$

where μ_A (μ_B) is the chemical potential of the molecules of species A (B). Moreover, N_{AA} , N_{AB} , and N_{BB} are the numbers of A-A, A-B, and B-B pairs of molecules, respectively, in a given configuration S on the lattice. Explicit expressions for these quantities were derived in Ref. [30]. Equilibrium states of our model are characterized by the grand potential density ω related to the partition function of the grand canonical ensemble Ξ according to [22]

$$\Xi(T, \mathcal{N}, \mu_A, \mu_B) = \sum_S \exp\left[-\frac{\mathcal{H}(S)}{k_B T}\right] \equiv \exp\left(-\frac{\mathcal{N}\omega}{k_B T}\right), \quad (2.3)$$

where T denotes temperature, and k_B is Boltzmann's constant.

To proceed, we introduce a mean-field approximation for the exact Hamiltonian given in Eq. (2.2). It consists of mapping the occupation-number *vector* S onto two scalar quantities (i.e., order parameters) by introducing (see Ref. [30] for details)

$$\rho \equiv \frac{1}{\mathcal{N}} \sum_{k=1}^{\mathcal{N}} s_k^2, \quad (2.4a)$$

$$\rho m \equiv \frac{1}{\mathcal{N}} \sum_{k=1}^{\mathcal{N}} s_k, \quad (2.4b)$$

where $\rho \in [0, 1]$ is the mean density of the lattice fluid (in units of ℓ^3) and $m \in [-1, 1]$ is the (dimensionless) miscibility parameter. As one can verify from the definition in Eq. (2.4b), $m = -1$ if all nonempty cells of the lattice are occupied by molecules of species B (i.e., $s_k^2 = -s_k$), whereas $m = +1$ if they are occupied by molecules of species A instead ($s_k^2 = s_k$). In the thermodynamic limit $\mathcal{N} \rightarrow \infty$, both order parameters become continuous on their respective domains. The advantage of replacing $\mathcal{H}(S)$ by its mean-field analog $\mathcal{H}_{\text{mf}}(\rho, m)$ is that we can derive an analytic expression for ω . Details of this derivation can be found in Refs. [30,31]. We finally obtain

$$\begin{aligned}
\omega(T, \mu, \Delta\mu)|_{\rho, m} &= -\mu\rho - \Delta\mu\rho m + k_B T \left\{ \rho \ln \rho + (1-\rho) \ln(1-\rho) \right. \\
&\quad \left. + \frac{\rho}{2} [(1+m) \ln(1+m) + (1-m) \ln(1-m)] \right\} \\
&\quad - \frac{3\rho^2}{4} [\epsilon_{AA}(1+m)^2 + 2\epsilon_{AB}(1+m)(1-m) \\
&\quad + \epsilon_{BB}(1-m)^2], \tag{2.5}
\end{aligned}$$

where the term proportional to T represents the entropic contribution to the grand-potential density and intermolecular interactions are accounted for by the last term in Eq. (2.5) (proportional to ρ^2). The first two terms on the right side of Eq. (2.5) arise because of the coupling of the lattice fluid to a (an infinitely large) reservoir of matter where, in particular,

$$\mu \equiv \frac{\mu_A + \mu_B}{2} + k_B T \ln 2, \tag{2.6a}$$

$$\Delta\mu \equiv \frac{\mu_A - \mu_B}{2} \tag{2.6b}$$

are thermodynamic fields coupling to the mean density [see Eq. (2.6a)] and concentration of the binary mixture [see Eq. (2.6b)], respectively. Note that we have included a trivial contribution $k_B T \ln 2$ in our definition of μ , which arises on account of the different “color” associated with molecules of species A and B, that is their formal distinguishability because of the labels “A” or “B.” If one prefers a more physical interpretation of this scenario we may identify these “labels” as internal, spinlike degrees of freedom following an earlier suggestion of Pini *et al.* [28].

B. Gibbs’ phase rule and its consequences

In principle, for a given set of values of the thermodynamic fields T , μ , and $\Delta\mu$, ω represents a complex surface in order-parameter (i.e., ρ - m) space which may have several minima corresponding to thermodynamic phases. By analogy with mechanical systems, these minima refer to stable phases $\mathcal{P}^\alpha = (\rho^\alpha, m^\alpha)$, where ρ^α and m^α are order-parameter values at the minimum pertaining to phase \mathcal{P}^α . For most combinations of the thermodynamic fields, one minimum will be the global one referring to a thermodynamically (i.e., globally) stable phase, whereas the others are only locally stable (i.e., metastable). However, under suitable conditions (i.e., in certain regions of thermodynamic state space) the global minimum may be degenerate in the sense that two or more phases are characterized by the same value of the associated grand-potential density at these minima. In this case, two or more thermodynamically stable phases coexist.

The number of coexisting phases p as well as the dimensionality f of the geometrical object describing a particular kind of phase coexistence are determined by the celebrated Gibbs phase rule which may be stated as

$$f = c + 2 - p \tag{2.7}$$

for a mixture of c components. We note in passing that f is usually referred to as the “number of degrees of freedom” in most standard physical chemistry textbooks [32]. However, here one gains more insight if one adopts an interpretation of f as the dimension of the geometric object along which phase coexistence arises. Because of this interpretation, we conclude that $f \geq 0$ to be geometrically (and therefore physically) meaningful because a geometric object of negative dimension is inconceivable. Specializing immediately to binary mixtures ($c=2$) this, in turn, requires p to satisfy the inequality $p \leq 4$.

Obviously, the simplest case is the one in which a pair of phases coexists ($p=2$). From Eq. (2.7), we infer that $f=2$, that is the two phases coexist along a two-dimensional surface in T - μ - $\Delta\mu$ space. Let us now impose one additional constraint on points pertaining to the coexistence surface, namely, that

$$\left(\frac{\partial^2 \omega}{\partial \mu^2} \right)_T = \left(\frac{\partial^2 \omega}{\partial \Delta \mu^2} \right)_T = 0. \tag{2.8}$$

Hence, we are looking for those points on the coexistence surface at which the two phases become critical. Note that points on the coexistence surface already satisfy

$$\left(\frac{\partial \omega}{\partial \mu} \right)_T = \left(\frac{\partial \omega}{\partial \Delta \mu} \right)_T = 0, \tag{2.9}$$

that is these points correspond to minima of ω in a thermodynamic state space. Together with Eq. (2.8), the previous expression establishes the condition for criticality of the binary mixture. Obviously, the set of critical points must form a *line* on the coexistence *surface*. Alternatively, we may replace the constraint stated in Eq. (2.8) by another one, namely






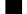

$$m(\mathcal{P}^\alpha) = m(\mathcal{P}^\beta). \tag{2.10}$$

Because Eqs. (2.9) and (2.10) are supposed to hold simultaneously, we are now dealing with another set of points (i.e., a line) on the coexistence surface where the composition (i.e., the concentration) of the coexisting phases α and β is the same. Coexisting phases complying with the constraint in Eq. (2.10) are termed “azeotrope.”

If three phases are in coexistence ($p=3$), it follows from Gibbs’ phase rule that these may be represented by a line of points in T - μ - $\Delta\mu$ space because $f=1$. This line is usually referred to as triple line. We may also envision a situation where any pair of the three coexisting phases become critical, whereas the remaining third phase stays noncritical. Hence, we impose Eq. (2.8) in addition to the threefold degeneracy of the global minimum of the grand-potential density. As a consequence, one *point* on the triple *line* may satisfy both conditions and this point is usually termed a “critical end point” (CEP). Alternatively, one may impose Eq. (2.10) to the triple line. By the same token, an azeotropic *point* may exist along the triple *line* at which both triple and azeotropic lines intersect.

Because $p \leq 4$, we may also have a quadruple *point* at

TABLE I. Geometrical nature of phase coexistences and symbols used to distinguish them in subsequent figures.

Coexisting phases	Noncritical phases			Critical phases		CEP	Azeotropy
	2	3	4	2	3	3	2
Dimension f^a	2	1	0	1	0	0	1
Object	coexistence surface	triple line	quadruple point	critical line	tricritical point	critical end point	azeotropic line
Symbol							

^aSee Eq. (2.7).

which the global minimum of the grand-potential density exhibits a fourfold degeneracy, that is four phases of the binary mixture may coexist at an isolated point in T - μ - $\Delta\mu$ space, because here Gibbs' phase rule leads to $f=0$. We summarize these results in Table I.

A somewhat special case also listed in Table I is the one termed the "tricritical point" (TCP). Here we are dealing with three phases that become critical simultaneously. However, from the above discussion, it turns out that three coexisting phases in a binary mixture form a line in T - μ - $\Delta\mu$ space because $f=1$. If all three phases become critical, we need to impose *two* more constraints of the form given in Eq. (2.8) for any two pairs of phases that become critical *independently*, which implies criticality of the remaining pair of the triplet. However, our discussion above already showed that applying one additional constraint of the form given in Eq. (2.8) means that we are searching for a *point* on the triple line. If we impose a second independent condition to this point, we would, in fact, be searching for a geometric object of dimension $f=-1$, which is inconceivable. Therefore, for purely geometric reasons, a tricritical point should not exist in binary mixtures but appear only in ternary and higher-order multicomponent mixtures, where we would have three-phase coexistence on a hypersurface of dimension $f\geq 2$. However, if the criticality of one of the two phases *depends* on the fact that one of the other two become critical simultaneously because of some special inherent symmetry, we are, in fact, imposing only a single *independent* additional constraint on the mixture. In this special case, a tricritical point may exist somewhere along the triple line.

One immediately realizes that one example, for such a special situation is the symmetric binary mixture in which $\epsilon_{AA}=\epsilon_{BB}$ and $\Delta\mu=0$ [17,28,30]. In this case, A- and B-rich demixed liquid phases can only be distinguished on account of the color of the molecules forming one or the other mixture component. Following again the interpretation put forth by Pini *et al.* [28], the color of molecules of different species may be viewed as a "...spinlike variable in addition to translational degrees of freedom so that their mutual interaction depends both on their relative position and on their 'internal' state, namely whether the interacting particles belong to the same species or not." In such a symmetric mixture, both demixed liquid phases may coexist with a gaseous phase and eventually become critical. However, on account of the sym-

metry of this mixture type, this cannot happen *independently*. Consequently, a point may exist at which A- and B-rich demixed liquid phases and a gaseous phase become critical simultaneously. In the light of this discussion, the existence of tricritical points turns out to be merely a consequence of a special symmetry inherent in the model system. We shall return to this issue, which is central to this work, in greater detail in Sec. IV, where we discuss our findings in a broader context.

C. Limiting cases

1. Pure lattice fluid as a degenerate case

However, before attending to that discussion, it seems instructive to consider briefly a number of limiting cases of Eq. (2.5). These limiting cases will turn out to be relevant to the subsequent analysis of the topology of complete (three-dimensional) phase diagrams to be presented in Sec. III. We begin with the pure fluid as a reference system which is characterized by

$$\epsilon_{AA} = \epsilon_{AB} = \epsilon_{BB} = \bar{\epsilon}, \quad (2.11a)$$

$$\mu_A = \mu_B. \quad (2.11b)$$

With this notation, we obtain from Eqs. (2.5) and (2.6a) the simpler expression

$$\omega = -\mu\rho + k_B T \{ \rho \ln \rho + (1-\rho) \ln(1-\rho) \} + \frac{\rho k_B T}{2} \{ (1+m) \times \ln(1+m) + (1-m) \ln(1-m) \} - 3\bar{\epsilon}\rho^2. \quad (2.12)$$

In order to minimize ω with respect to ρ and m , one can show that for any constant ρ $\partial\omega/\partial m=0$ only for $m=0$ because the term $\ln[(1+m)/(1-m)]$ vanishes only for this value of m . Hence, we are dealing with stable phases that are always mixed according to the definition of m in Eq. (2.4b). For $m=0$, on the other hand, Eq. (2.12) may be simplified to give

$$\omega = -\mu\rho + k_B T \{ \rho \ln \rho + (1-\rho) \ln(1-\rho) \} - 3\bar{\epsilon}\rho^2, \quad (2.13)$$

which is nothing but the well-known expression for the grand-potential density of the pure lattice fluid [22]. In Eq.

(2.13), ω turns out to be symmetric with respect to ρ and $1-\rho$ if and only if $\mu = -3\bar{\epsilon}$. For this value of the chemical potential, one can show easily that ω possesses two minima (located at ρ and $1-\rho$) for all $0 \leq k_B T \leq \frac{3}{2}\bar{\epsilon}$. Coexisting gas and liquid phases are then characterized by this double minimum in ω at $\mu_x = -3\bar{\epsilon}$, where subscript “x” is used here and below to indicate the value of μ at coexistence. Hence, we observe gas+liquid coexistence along the line $\mu_x = -3\bar{\epsilon}$ in $T-\mu$ space, which ends at the critical point, where

$$\left(\frac{\partial\omega}{\partial\rho}\right)\Big|_{T=T_c, \mu=\mu_c} = \left(\frac{\partial^2\omega}{\partial\rho^2}\right)\Big|_{T=T_c, \mu=\mu_c} = 0. \quad (2.14)$$

From the previous expression, $k_B T_c = \frac{3}{2}\bar{\epsilon}$ and $\mu_c = -3\bar{\epsilon}$ follow without further ado.

2. The limit $\Delta\mu \rightarrow \pm\infty$

As we already pointed out in Sec. II A, the field $\Delta\mu$ couples directly to the concentration of the mixture [see also Eq. (2.6b)]. For large positive values of $\Delta\mu$ the term $-\Delta\mu\rho m$ in Eq. (2.5), which is linear in m ($\rho = \text{const}$), causes the minimum of ω to be shifted to higher values of m as $\Delta\mu$ increases. Hence, the limit $\Delta\mu \rightarrow +\infty$ (i.e., $\mu_B \rightarrow -\infty$) corresponds to a binary mixture in which component B is present only at infinite dilution, that is $m \rightarrow +1$. Therefore, at any finite value of μ_A , we may replace Eq. (2.5) by the simpler expression

$$\begin{aligned} \lim_{\mu_B \rightarrow -\infty} \omega(T, \mu, \Delta\mu) &= \omega(T, \mu_A) \\ &= -\mu_A \rho + k_B T \{ \rho \ln \rho + (1-\rho) \ln(1-\rho) \} \\ &\quad - 3\epsilon_{AA} \rho^2, \end{aligned} \quad (2.15)$$

where we also used Eqs. (2.6a) and (2.6b). Hence, comparing Eq. (2.15) with the corresponding one for the pure lattice fluid [see Eq. (2.13)], we notice that the functional dependence of the grand-potential density on T and ρ is identically the same. Hence, we would expect coexistence between liquid and gaseous pure A fluids in the limit $\Delta\mu \rightarrow +\infty$ ($\mu_B \rightarrow -\infty$) along a coexistence line

$$\mu_A = -3\epsilon_{AA} \quad (2.16)$$

terminating at a critical point C_A at

$$k_B T_c^A = \frac{3}{2}\epsilon_{AA}, \quad (2.17)$$

which follows from the parallel analysis of Eq. (2.13) in Sec. II C 1. Transforming back to our original thermodynamic fields, T , μ , and $\Delta\mu$, we can recast Eq. (2.16) with the aid of Eqs. (2.6) as

$$\Delta\mu_x = -\frac{3}{2}\epsilon_{AA} - \frac{\mu_B}{2}, \quad (2.18a)$$

$$\mu_x = -\frac{3}{2}\epsilon_{AA} + \frac{\mu_B}{2} + k_B T \ln 2, \quad (2.18b)$$

which are valid in the limit $\mu_B \rightarrow -\infty$ for all $0 \leq k_B T < \frac{3}{2}\epsilon_{AA}$. Hence, Eqs. (2.18) represent the full line in Fig. 1 ending at

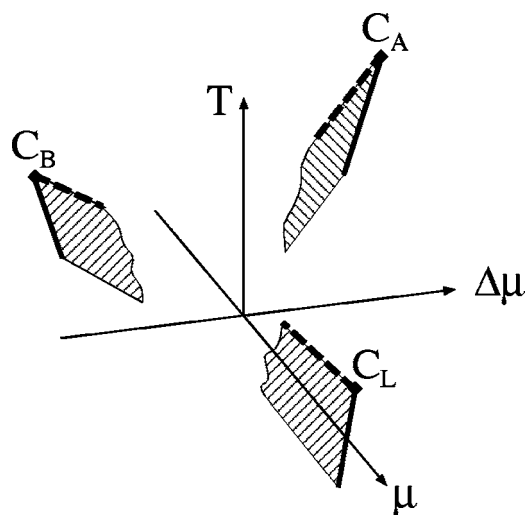


FIG. 1. Schematic representation of phase diagram of binary mixtures in limiting cases $\Delta\mu \rightarrow \pm\infty$ and $\mu \rightarrow +\infty$ discussed in Secs. II C 2 and II C 3. Thick lines connecting C_α ($\alpha = A, B, \text{ or } L$) to a point in the $\mu-\Delta\mu$ plane are coexistence lines of the *effective* pure lattice fluid. C_L exists only for mixtures obeying Eq. (2.27).

the critical point C_A .

However, the above considerations are not only valid in the limit $\mu_B \rightarrow -\infty$ but also for *finite* but very large negative values of μ_B , such that $\Delta\mu \gg 0$. To see that, we add Eqs. (2.18) and obtain after rearranging terms

$$\mu_x = -3\epsilon_{AA} - \Delta\mu_x + k_B T \ln 2 \quad (\Delta\mu \gg 0) \quad (2.19)$$

for phase coexistence between A-rich liquid and gas. The reader should note that since μ_x depends linearly on both $\Delta\mu_x$ and T , Eq. (2.19) defines a plane schematically depicted in Fig. 1 by the hatched area forming an angle of $\pi/4$ with the positive $\Delta\mu$ axis. One can also verify from Eq. (2.19) that this plane is bent toward more positive μ values as T increases.

In the opposite case, namely if $\Delta\mu \ll 0$ (i.e., $\mu_A \ll 0$), it is straightforward to demonstrate that

$$\mu_x = -3\epsilon_{BB} + \Delta\mu_x + k_B T \ln 2 \quad (\Delta\mu \ll 0) \quad (2.20)$$

by the same token as before but for $m \rightarrow -1$. Hence, Eq. (2.20) defines a plane at which B-rich liquid and gas coexist. As can be seen in Fig. 1, in the limit $\Delta\mu \rightarrow -\infty$, this coexistence plane terminates at the critical line ending at the critical point C_B whose temperature is given by

$$k_B T_c^B = \frac{3}{2}\epsilon_{BB}. \quad (2.21)$$

Similar to the previous case the coexistence plane forms an angle of $-\pi/4$ with the negative $\Delta\mu$ axis.

3. The limit $\mu \rightarrow \infty$

Next, we consider the case in which $\Delta\mu$ remains finite but μ tends to infinity. The structure of Eq. (2.5) requires that in this limit $\rho \rightarrow 1$, so we are dealing with liquid phases. Introducing the mole fraction of species A via

$$x_A \equiv \frac{1+m}{2}, \quad (2.22)$$

we may rewrite Eq. (2.5) as

$$\begin{aligned} \lim_{\mu \rightarrow +\infty} \omega(T, \mu, \Delta\mu) &= -\mu - \Delta\mu(2x_A - 1) \\ &+ k_B T [x_A \ln x_A + (1-x_A) \ln(1-x_A) + x_A \ln 2] \\ &- 3[(\epsilon_{AA} - 2\epsilon_{AB} + \epsilon_{BB})x_A^2 + 2(\epsilon_{AB} - \epsilon_{BB})x_A + \epsilon_{BB}]. \end{aligned} \quad (2.23)$$

Introducing

$$C \equiv -\mu + \Delta\mu - 3\epsilon_{BB}, \quad (2.24a)$$

$$\bar{\mu} \equiv 2\Delta\mu + 6(\epsilon_{AB} - \epsilon_{BB}) - k_B T \ln 2, \quad (2.24b)$$

$$\epsilon_L \equiv \epsilon_{AA} - 2\epsilon_{AB} + \epsilon_{BB}, \quad (2.24c)$$

we can rewrite Eq. (2.23) as

$$\begin{aligned} \lim_{\mu \rightarrow +\infty} \omega(T, \mu, \Delta\mu) &= C - \bar{\mu}x_A + k_B T [x_A \ln x_A + (1-x_A) \ln(1-x_A)] - 3\epsilon_L x_A^2, \end{aligned} \quad (2.25)$$

which turns out to be again of the same functional form as Eq. (2.13) except for the trivial constant C , which is inconsequential for the determination of minima. Comparison between Eq. (2.25) and Eqs. (2.13) and (2.15) also shows that ρ has been replaced by x_A in the *liquid* phase as the relevant order parameter, where now ϵ_L determines the mean attractiveness between molecules of the binary mixture [see Eq. (2.24c)]. Hence, because of this and because of the functional equivalence between Eqs. (2.13) and (2.25), we are anticipating the existence of a third coexistence line for

$$\bar{\mu}_x = -3\epsilon_L, \quad (2.26a)$$

$$k_B T \leq k_B T_c^L = \frac{3}{2}\epsilon_L, \quad (2.26b)$$

now referring to coexisting A- and B-rich *liquid* phases. Equation (2.26b) has an immediate consequence which we note for future reference in Sec. III. Since T in Eq. (2.26b) is obviously positively semidefinite, the inequality prompts us to conclude that liquid+liquid phase coexistence will arise only if [see Eq. (2.24c)]

$$\epsilon_{AB} < \frac{1}{2}(\epsilon_{AA} + \epsilon_{BB}). \quad (2.27)$$

However, strictly speaking, the above analysis is valid only in the limit $\mu \rightarrow \infty$. For large but *finite* μ , we realize that the coexistence *line* will be replaced by a coexistence *plane* by the same token as before (see Sec. II C 2). Using Eqs. (2.26a) and (2.24b), this plane in T - μ - $\Delta\mu$ space is given by the condition

$$\begin{aligned} \Delta\mu_x &= -\frac{3}{2}\epsilon_L + \frac{k_B T}{2} \ln 2 - 3(\epsilon_{AB} - \epsilon_{BB}) \\ &= -\frac{3}{2}(\epsilon_{AA} - \epsilon_{BB}) + \frac{k_B T}{2} \ln 2 \quad (\mu \geq 0), \end{aligned} \quad (2.28)$$

which is independent of μ and therefore parallel to the μ axis as indicated in Fig. 1. In that figure the limiting critical point is labeled C_L .

It is clear that for coexistence surfaces to be physically meaningful they must be represented by ordinary contiguous domains, that is they must not contain any ‘‘holes.’’ Hence, the topology of the phase diagrams of binary mixtures will depend on two conditions, namely, (1) how many coexistence surfaces exist [i.e., depending on whether or not liquid+liquid phase coexistence occurs, see Eq. (2.27)] and (2) the way in which these coexistence surfaces are connected in the space spanned by T , μ , and $\Delta\mu$. Hence, the topology of phase diagrams depends on possible ways in which the geometrical elements identified in Table I may be combined.

III. RESULTS

A. Parameter space

Henceforth, we shall express all quantities in the customary dimensionless units, that is temperature is given in units of ϵ_{AA}/k_B , energies in units of ϵ_{AA} , and densities in units of ℓ^3 . Since we are dealing with binary mixtures composed of molecules of equal size, this leaves us with only two *independent* model parameters describing the attractions between molecules of both species, namely ϵ_{BB} and ϵ_{AB} (since $\epsilon_{AA}=1$ in the dimensionless units). However, following the work by van Konynenburg and Scott [4], we introduce a more convenient parametrization via

$$\zeta \equiv \frac{1 - \epsilon_{BB}}{1 + \epsilon_{BB}}, \quad (3.1a)$$

$$\Lambda \equiv 1 - \frac{2\epsilon_{AB}}{1 + \epsilon_{BB}}. \quad (3.1b)$$

In the still vast parameter space characterizing binary mixtures, we focus on a somewhat narrow but most interesting region in which ζ is small, that is $\epsilon_{BB} \approx 1$ (i.e., $\epsilon_{BB} \approx \epsilon_{AA}$ in absolute units) which causes C_A and C_B to be distinct but rather similar. In addition, we do not consider mixtures characterized by $\Lambda < 0$, because these mixtures do not exhibit liquid+liquid phase separation even for large μ [see Eq. (2.27)]. Consequently, we concentrate here on the more interesting cases characterized by $\Lambda > 0$ for which C_L exists because the inequality Eq. (2.27) applies. We emphasize, however, that we also verified the existence of mixtures of a type existing only for combinations of ζ and Λ outside our present range of interest [33]. For example, our model is capable of reproducing mixtures of types IV and V of the van Konynenburg and Scott classification scheme (see Fig. 1 of Ref. [4]).

Henceforth, we shall classify our model mixtures according to the scheme proposed by van Konynenburg and Scott

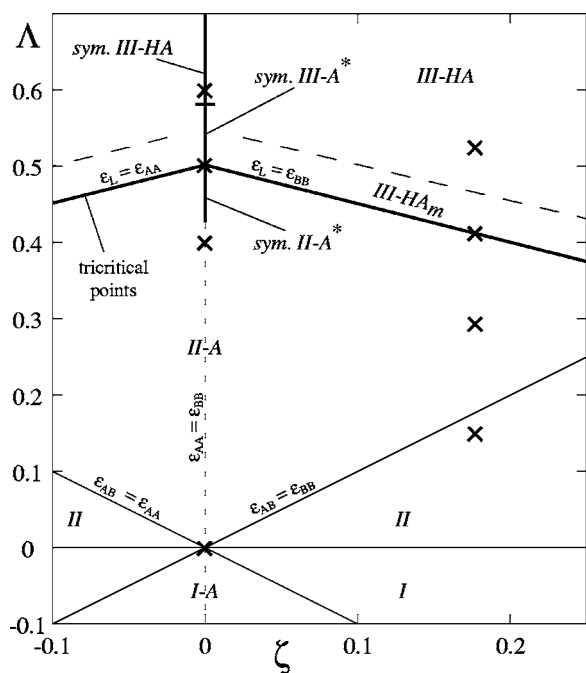


FIG. 2. Partial phase diagram for mixtures composed of molecules of equal size. Solid lines separate regions of the ζ - Λ plane [see Eqs. (3.1)] characterized by mixtures of a specific type following the classification scheme introduced in Ref. [4] (see text). Complete phase diagrams are presented in this work for the cases indicated by \times . Vertical dashed line (---) [$\zeta=0$, see Eq. (3.1a)] refers to symmetric mixtures of various types whereas the long dashed line (—) demarcates boundary between mixtures of type III-HA and III-HA_m. Limits of azeotropy are indicated by lines $\Lambda = \pm \zeta$. Thick solid lines refer to systems exhibiting one TCP.

[4] and adopted later by Deiters and Pegg [10]. Their classification scheme is illustrated in Fig. 2, where we identify regions of distinct phases indicated in the figure and separated by characteristic lines. The diagram is symmetric with respect to the Λ axis where the mirror image obtains if A and B components are interchanged, so that only cases for which $\zeta > 0$ need to be considered explicitly. Thick solid lines in Fig. 2 demarcate systems exhibiting one TCP. On account of the different systems considered by van Konynenburg and Scott [4], Deiters and Pegg [10], and us, we have adjusted the position of these lines from the corresponding partial phase diagram presented by van Konynenburg and Scott (their Fig. 1) by making sure that our symmetric mixtures ($\zeta=0$) pertain to the correct classes indicated in Fig. 2.

The most important mixture classes in the context of our work are labeled I, II, II-A, and III-HA (see Fig. 2). Their main features can be summarized as follows. Except for mixtures of type I, all others exhibit three critical points in the limits $\mu \rightarrow +\infty$, $\Delta\mu \rightarrow \pm\infty$, namely C_A , C_B , and C_L at which critical lines end (see Secs. II C 2 and II C 3). In mixtures of type I, C_L does not exist because the inequality Eq. (2.27) is violated for $\Lambda < 0$ so that liquid+liquid phase separation cannot occur (see Sec. II C 3). Thus, mixtures of type I exhibit a single critical line connecting C_A and C_B . Mixtures of type I-A are characterized by an additional azeotropic line [see Eq. (2.10)] intersecting the critical line at a temperature

higher than that at either C_A or C_B (negative azeotrope).

Mixtures of type II exhibit liquid+liquid phase separation. They have one critical line connecting C_A and C_B and a second one connecting C_L to some CEP. Above the line $\Lambda = \pm \zeta$ (i.e., $\epsilon_{AB} = \epsilon_{BB}$ or $\epsilon_{AB} = \epsilon_{AA}$) type-II mixtures show an additional azeotropic line (positive azeotrope). This is indicated by the suffix “-A” in the appropriate region in Fig. 2.

Binary mixtures of type III-HA (and III-HA_m) are distinctly different from the other two types. Here one critical line connects C_A to C_L and a second one ties C_B to some CEP. Along the latter, T_c decreases monotonically thus giving rise to so-called “heteroazeotropic” behavior [1]. The difference between mixtures of types III-HA and III-HA_m is that, for the latter, the pressure along the critical line going from C_A and C_L passes through a local maximum and minimum before increasing continuously as one approaches C_L .

B. Symmetric mixtures

We begin the discussion of specific *complete* phase diagrams with symmetric mixtures which are realized by setting $\zeta=0$ (see Fig. 2).

1. Almost “simple” fluids

For pedagogic reasons, we first focus on an almost trivial case characterized by $\Lambda=0$. In this case, we may rewrite Eq. (2.5) (in dimensionless units, see Sec. III A) as

$$\omega(T, \mu, \Delta\mu) = -\mu_{\text{art}}\rho + T[\rho \ln \rho + (1-\rho)\ln(1-\rho)] - 3\rho^2, \quad (3.2)$$

where the artificial chemical potential is defined as

$$\mu_{\text{art}} \equiv \mu + \Delta\mu m + \frac{T}{2}[(1+m)\ln(1+m) + (1-m)\ln(1-m)]. \quad (3.3)$$

Comparison of Eqs. (3.2) and (2.13) reveals that we are dealing with an effective pure fluid, where, however, the chemical potential μ_{art} depends on T and m [22]. Thus, in the present case, we expect gas+liquid coexistence for $T \leq \frac{3}{2}$ and $\mu_{\text{art}} = -3$ (see Sec. II C 1). For constant $T \leq \frac{3}{2}$ and for $\mu_{\text{art}} = -3$ in Eq. (3.3), we realize that μ becomes a function of $\Delta\mu$ whereas the value of m is determined by the condition $\mu_{\text{art}} = -3$. Therefore, we have isothermal lines of gas+liquid coexistences (i.e., different densities of coexisting phases) with m being equal in both phases. In other words, we have an azeotrope at *every* single point on the coexistence surface according to the definition in Eq. (2.10). The mixture is, therefore, a transition case between mixtures of types I *without* azeotropy and I-A with a single *line* of azeotropic points pertaining to the coexistence surface. Figure 3 shows the coexistence surface in T - μ - $\Delta\mu$ space for the present situation. Dashed-dotted lines indicate isotherms of two-phase coexistence. Three different regions are clearly discernible: for low μ the gas phase (G) is stable behind the surface. At sufficiently high μ , we also see a stable demixed A-rich liquid phase for large $\Delta\mu$, whereas the demixed B-rich liquid phase is stable at low values of $\Delta\mu$. The coexistence surface

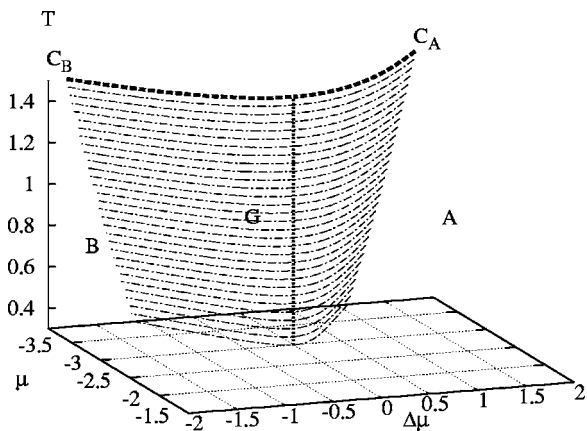


FIG. 3. Phase diagram for the case $\zeta=0$, $\Lambda=0$ in $T-\mu-\Delta\mu$ space where G, A, and B refer to one-phase regions of gaseous and A-rich and B-rich liquid mixtures, respectively. Gas+liquid critical points of pure A(B) fluids are labeled C_A (C_B) (see Table I for symbols and line styles). The vertical dotted line represents the case $\Delta\mu=0$.

terminates at the critical line connecting the critical points C_A and C_B of the pure A and B fluids, respectively, which is characteristic of type I mixtures. The temperature along this critical line $T_c = \frac{3}{2}$ is independent of μ and $\Delta\mu$. We note in passing that the vertical dotted line represents the corresponding phase diagram of a pure fluid whose grand-potential density, we recover from Eqs. (3.2) for $\Delta\mu=0$ which implies $m=0$ so that $\mu_{art}=\mu$.

2. $\Lambda=0.4$

Let us now promote demixing by changing Λ to 0.4 [see Eq. (3.1b)]. The corresponding complete phase diagram is presented in Fig. 4. From the plot in Fig. 4, we notice that the increased tendency of the mixture to decompose adds a new coexistence surface that did not appear for the previously discussed case (see Fig. 3). Across this surface decomposed A-rich and B-rich liquid phases coexist. The surface is bounded by a critical line extending toward C_L with increasing $\mu \rightarrow +\infty$ as discussed in Sec. II C 3. This coexistence

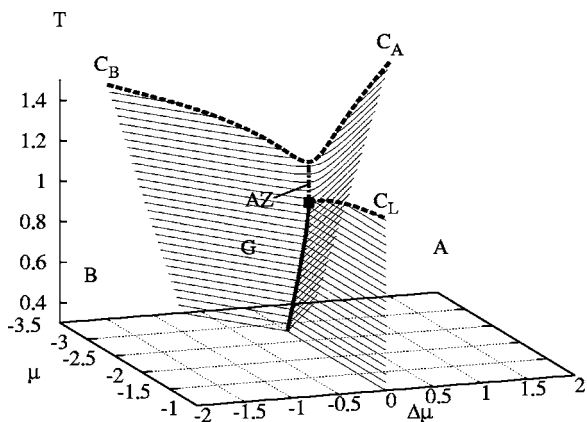


FIG. 4. As Fig. 3, but for $\Lambda=0.4$. Symbols C_L and AZ refer to the liquid+liquid critical point in the limit $\mu \rightarrow \infty$ (see Sec. II C 3) and a line of azeotropic points (see Table I for symbols and line styles).

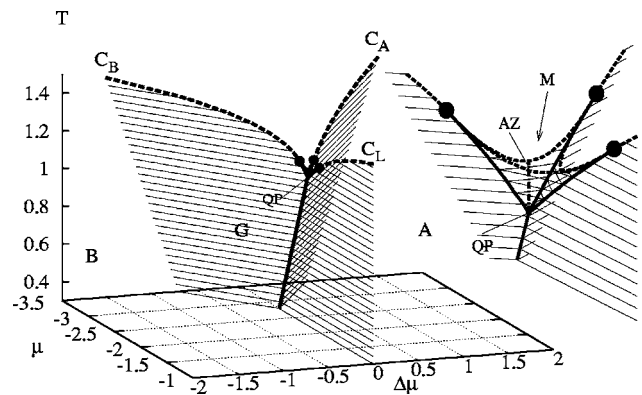


FIG. 5. As Fig. 4, but for $\Lambda=0.5$. The symbol QP refers to the quadruple point. The plot on the right side is an enlargement showing in addition a region of mixed liquid phases (M) and a line of azeotropic points (AZ) (see Table I for symbols and line styles).

surface joins the one corresponding to coexistence between both A-rich liquid and B-rich liquid and gas. However, because the critical line for the liquid+liquid coexistence is located at a temperature which is lower than that of the critical line connecting C_A and C_B , a CEP must exist at which the critical line starting at C_L connects to the coexistence surface between gas and demixed (A-rich and B-rich) liquid.

Below the CEP, the two surfaces are connected along a triple line, which turns into an azeotropic line above the temperature of the CEP. This line, for which $m=0$, terminates at the critical line between C_A and C_B bounding the second coexistence surface. The azeotropic line terminates at the minimum of this critical line so that we are dealing with positive azeotropy in Fig. 4.

The topology just discussed pertains to the class of symmetric II-A systems (see Fig. 2), which exists over the range $0 \leq \Lambda \leq 0.42$. Mixtures of this type have also been predicted on the basis of semiempirical equations of state [4,10]. More recently, Wilding also verified this type of mixture in a Monte Carlo study for $\Lambda=0.3$ [18], where we reemphasize that in none of these earlier works [4,10,18] complete phase diagrams were presented.

3. $\Lambda=0.5$

If we further enhance the tendency of the mixture to decompose by setting $\Lambda=0.5$, the topology of the corresponding complete phase diagram changes markedly as the plot in Fig. 5 illustrates. Now the three critical points C_A , C_B , and C_L have identical temperatures as one can verify from Eqs. (3.1), (2.17), (2.21), (2.24c), and (2.26b), because $\epsilon_{AA}=\epsilon_{BB}=\epsilon_L$. As one would anticipate intuitively the phase diagram turns out to be quite symmetric in this case. This enhanced symmetry (with respect to the two previously discussed cases in Secs. III B 2 and III B 3) causes the triple line, at which the two coexistence surfaces merge, to trifurcate into three separate triple lines at a quadruple point (QP). Each one of these triple lines terminates at a separate TCP.

Each pair of TCPs is connected by a critical line such that a fourth one-phase region arises bounded by three coexistence surfaces that are themselves bounded by three triple

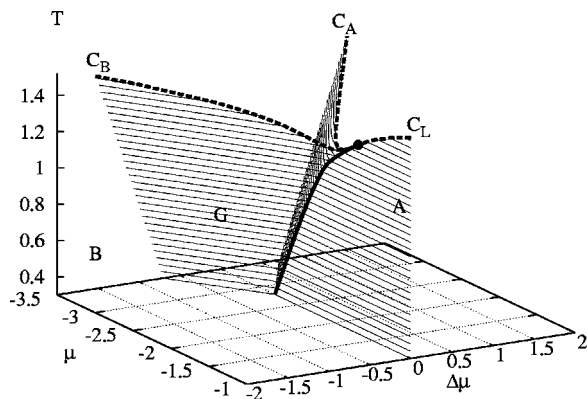


FIG. 6. As Fig. 4, but for $\Lambda=0.6$ (see Table I for symbols and line styles).

lines, the three critical lines, and the quadruple point as the enlargement in Fig. 5 reveals. This new one-phase region is identified as a “mixed” (M) phase because the stable liquid phase in this region is characterized by a relatively large density but small $|m|$. The new mixed phase coexists with both *demixed* A-rich and B-rich liquid phases for temperatures above and below that of the quadruple point and the three TCPs, respectively.

Across the coexistence surface between mixed liquid and gaseous phase, we observe a line of azeotropic points terminating at the respective critical line. The azeotropic line ends at the minimum of the critical line, that is we are again dealing with a case of positive azeotropy. A phase diagram of this topology has also been reported by Pini *et al.* (see Fig. 6(d) in Ref. [28]). It represents a transition state between symmetric II-A* and III-A* classes of systems (see Fig. 2 and Sec. IV). However, Pini *et al.* failed to recognize the presence of the azeotropic line displayed in Fig. 5 because they focused only on special (two-dimensional) projections rather than the full topology of the (three-dimensional) phase diagram [28].

4. $\Lambda=0.6$

Finally, we consider a system with an even stronger demixing tendency characterized by $\Lambda=0.6$. In this case, the fluid exhibits a tendency to decompose even at high temperatures as the plot in Fig. 6 shows. From the plot in that figure, we notice only a single TCP at which the triple line meets the two critical lines ending at C_A and C_B . At this TCP, all three lines have a common tangent. We also note that the two critical lines pass through a minimum before joining the triple line at the TCP. At the TCP, a third critical line starts ending at C_L . Mixed liquid phases or azeotropy as for $\Lambda=0.5$ are not observed here.

Referring back to the *partial* phase diagram plotted in Fig. 2, we realize that the present phase behavior pertains to the symmetric class III-HA according to van Konynenburg and Scott’s classification scheme [4]. A mixture of this sort has also been reported by Keskin *et al.* based upon an analysis of a lattice-fluid model where they focus, however, only on the critical lines [9] rather than the three-dimensional topology of the complete phase diagram.

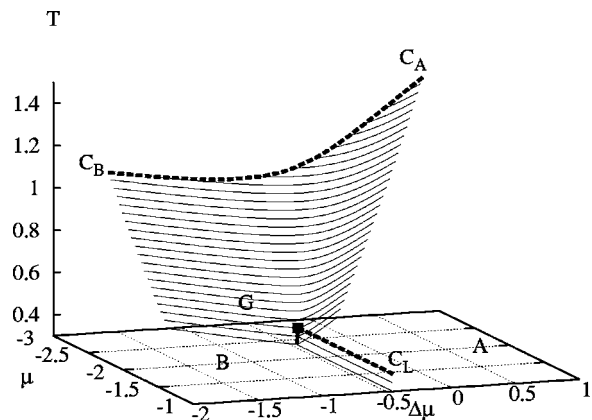


FIG. 7. Phase diagram for the case $\zeta=0.18$, $\Lambda=0.15$ in T - μ - $\Delta\mu$ space where G, A, and B refer to one-phase regions of gaseous and A-rich and B-rich liquid mixtures, respectively (see Table I for symbols and line styles).

C. Asymmetric binary mixtures

We now turn to a discussion of asymmetric binary mixtures, that is mixtures where $\epsilon_{AA} \neq \epsilon_{BB}$ [and consequently $\zeta \neq 0$, see Eq. (3.1a)]. Specifically, we consider mixtures for which $\zeta=0.18$ ($\epsilon_{BB}=0.7$, see Fig. 2). An immediate consequence of the asymmetry is a difference in temperature at the two critical points C_A and C_B . According to the discussion in Sec. II C 2, $T_c^A = \frac{3}{2}$, whereas $T_c^B = 1.05$ [see Eqs. (2.17) and (2.21)].

1. $\Lambda=0.15$

We begin this section with a system characterized by a rather small value of $\Lambda=0.15 < \zeta$. One might immediately expect that under these conditions, liquid+liquid phase separation should never occur because $\epsilon_{AB}=0.7225 > \epsilon_{BB}$. Hence, it is favorable both energetically and entropically for a molecule of species B to be surrounded by molecules of mixture component A rather than by other molecules of species B. However, as $\Delta\mu$ decreases [i.e., with increasing μ_B , see Eq. (2.6b)] the mixture accommodates more molecules of species B so that, in fact, decomposition into A- and B-rich liquid phases becomes possible as the plot in Fig. 7 shows in accord with the inequality in Eq. (2.27). The corresponding liquid+liquid coexistence surface is nearly orthogonal to the μ - $\Delta\mu$ plane and located along a line $\Delta\mu=-0.5$. The liquid+liquid critical line is almost independent of both $\Delta\mu$ and T with a critical temperature $T_c \approx T_c^L = 0.38$ [see Eqs. (2.24c), (2.26b), and (3.1)]. This critical temperature is also equal to the temperature of the CEP (on account of the temperature independence of the liquid+liquid critical line) at which the critical line terminates on the coexistence surface between gaseous and A- and B-rich liquid phases.

Further inspection of Fig. 7 reveals that the critical line connecting C_A and C_B varies monotonically. Therefore, we do not observe azeotropy (either positive or negative), and consequently, the present topography of the phase diagram is characteristic of mixture type II as we infer from Fig. 2.

2. $\Lambda=0.29$

If we now increase Λ to a value of 0.29 the situation is different from the one discussed previously in Sec. III C 1 in

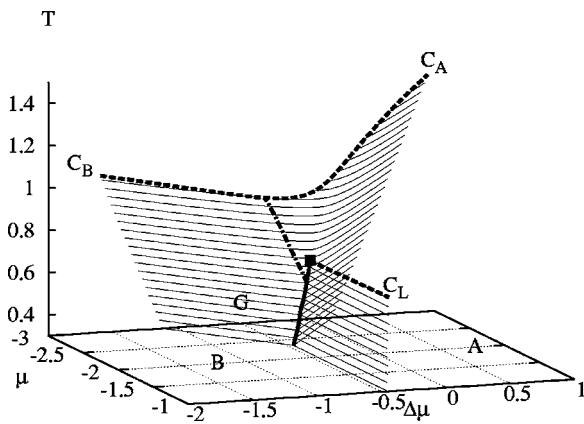


FIG. 8. As Fig. 7, but for $\Lambda=0.29$ (see Table I for symbols and line styles).

that the attraction between unlike molecules is weaker than that between like molecules of either species. Nonetheless, the phase diagram in the present case has features qualitatively similar to that presented in Fig. 7. However, the temperature at the CEP is substantially larger here than the corresponding one in Fig. 7. More importantly though is the fact that the critical line connecting C_A and C_B now passes through a minimum. As was seen for $\zeta=0$ before, this gives rise to azeotropy in the phase diagram plotted in Fig. 8. The line of azeotropic points is shifted to the left of the coexistence surface along which gaseous phases coexist with demixed liquid phases. Because of the topology of its phase diagram the present mixture still pertains to class II-A according to the classification scheme illustrated by the plot in Fig. 2.

A minor aspect that cannot be read off the plot in Fig. 8 concerns the fact that along the line of azeotropic points the composition of the mixture is nearly temperature independent characterized quantitatively by $m \approx -0.6$; that is, we are dealing with B-rich azeotropes.

3. $\Lambda=0.41$

As Λ increases to 0.41, the mixture exhibits an increasing tendency to decompose. Consequently, the critical line ending eventually at C_L is shifted to even higher T compared with both previously discussed cases as one can see in Fig. 9. For this value of Λ , it turns out that $\epsilon_{BB} = \epsilon_L$ [see Eq. (2.24c)] and hence $T_c^B = T_c^L = 1.05 < T_c^A = \frac{3}{2}$, so that the mixture exhibits a symmetry with respect to coexistence between gas and B-rich liquid (C_B) and coexistence between A- and B-rich liquids (C_L). Therefore, the two critical lines ending at C_L and C_B eventually merge with the triple line at a TCP now shifted toward C_A .

Moreover, the phase diagram plotted in Fig. 9 contains a short line of azeotropic points indicating that we are still in the azeotropic regime of the *partial* phase diagram plotted in Fig. 2. In fact, the present mixture is sort of a transition state between a mixture of type II-A and III-HA_m. The latter is inferred from a plot of the pressure P versus temperature in Fig. 10, because along the critical line from C_A to C_L the curve plotted in Fig. 10 passes through a maximum and a

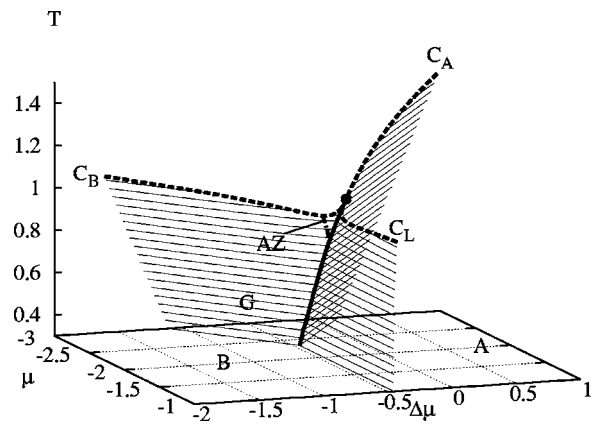


FIG. 9. As Fig. 7, but for $\Lambda=0.41$ (see Table I for symbols and line styles).

minimum before increasing monotonically as one approaches C_L [4]. Here the pressure is obtained from the usual expression (see, for example, Ref. [34])

$$\omega = -P. \tag{3.4}$$

4. $\Lambda=0.53$

In this case, the tendency to decompose in the liquid phase has risen to the extent that, similar to the *symmetric* mixture ($\zeta=0$) at $\Lambda=0.29$ [see Fig. 8] two of the three limiting critical points are connected by a single critical line. According to the plot in Fig. 11, these appear to be C_A and C_L in the present case; whereas in Fig. 8, the two critical points complying with this condition were C_A and C_B . Hence, in a certain sense, one may perceive the phase diagram plotted in Fig. 11 as being qualitatively equivalent to the one shown in Fig. 8 but rotated by an angle $3\pi/4$ in the μ - $\Delta\mu$ plane (see Sec. IV).

Finally, to make sure that the phase diagram plotted in Fig. 11 pertains to the class III-HA of van Konynenburg and Scott's classification scheme (see Fig. 2), we analyze a plot of P versus T in Fig. 12, which confirms our expectation,

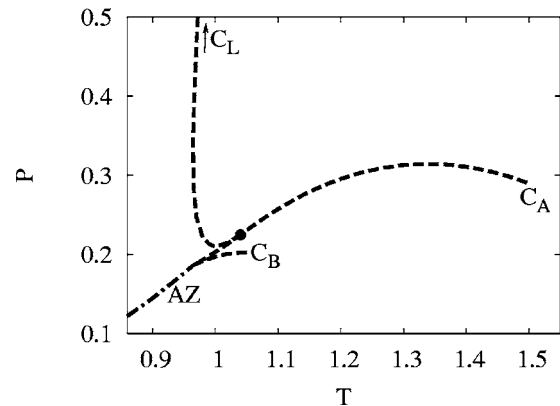


FIG. 10. Pressure P as function T along specific lines of the phase diagram plotted in Fig. 9 (see Table I for symbols and line styles).

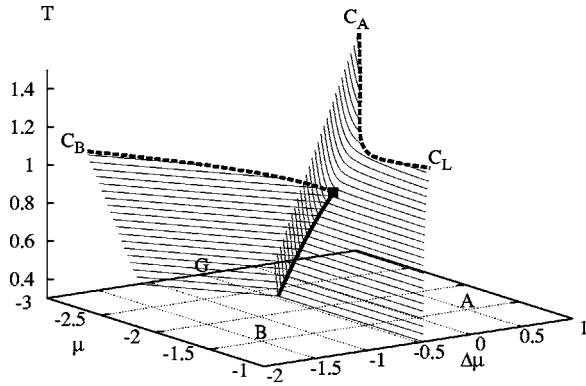


FIG. 11. As Fig. 7, but for $\Lambda=0.53$ (see Table I for symbols and line styles).

because in this case C_A and C_L are connected by a monotonically increasing (decreasing) critical line.

IV. DISCUSSION AND CONCLUSIONS

In this work, we focus on the topology of *complete* phase diagrams for symmetric and asymmetric binary mixtures. In the context of this work the terms “symmetric” and “asymmetric” refer to $\epsilon_{AA}=\epsilon_{BB}$ ($\zeta=0$) and $\epsilon_{AA}\neq\epsilon_{BB}$ ($\zeta>0$), respectively. From a discussion of Gibbs’ phase rule in the light of these systems, we argued in Sec. II B that in binary fluid mixtures, TCPs should not exist *in general*. The reason is that the condition of *independent* criticality of three pairs of phases all in coexistence with each other cannot be satisfied geometrically. This is because in thermodynamic state space three coexisting phases are represented by a (triple) line. Imposing one additional constraint on the set of points forming that line selects one of them (e.g., a CEP). This point cannot satisfy yet another *independent* condition of the sort stated in Eq. (2.8) *simultaneously*. In other words, we would be searching for a geometrically undefined object of dimension $f=-1$ by imposing Eq. (2.8) independently twice on points along the triple line.

Nevertheless, existence of TCPs in binary mixtures has been predicted by Furman and Griffiths [6], by van

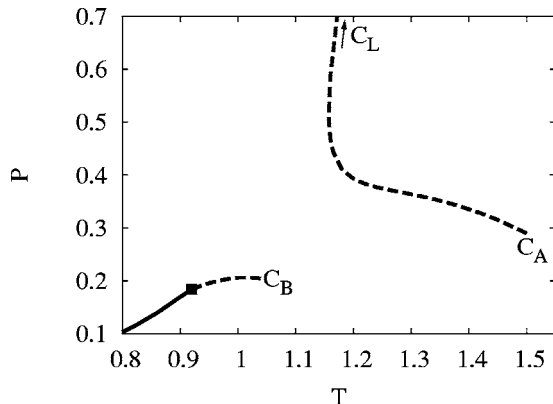


FIG. 12. Pressure P as function T along specific lines of the phase diagram plotted in Fig. 11 (see Table I for symbols and line styles).

Konynenburg and Scott [4], and subsequently verified by a number of others [7–12,28]. However, because in none of these previous studies the full topology of the phase diagram was considered, the crucial relation between special symmetries in the binary mixture and the existence of TCPs was not fully appreciated. This is because the overwhelming number of these earlier works was based upon semiempirical equations of state where it would be exceedingly hard to calculate the grand (or any other) thermodynamic potential which is the key quantity if one aims at constructing complete phase diagrams as in this work. On the contrary, our microscopic (i.e., molecular) approach permits a relatively easy access to ω . From a detailed investigation of complete phase diagrams constructed from ω , we demonstrate that TCPs may form if the two conditions of criticality imposed on points along a triple line are mutually dependent.

Such a situation arises, for example, if symmetric mixtures are concerned because if gas and A-rich liquid become critical, so must gas and B-rich liquid since molecules of both components are distinct only by their color. This causes C_A and C_B to be located at the same temperature $T_c^A=T_c^B=\frac{3}{2}$, so that the variation of the critical line between C_A and C_B is symmetric with respect to the plane $\Delta\mu=0$. If C_L is located at a temperature far lower than $T_c^A=T_c^B>T_c^L$, all three coexistence surfaces merge along a triple line ending at a CEP as illustrated by the plot in Fig. 4.

However, if C_L is located at a temperature above $T_c^A=T_c^B<T_c^L$, a different scenario becomes possible. This situation arises for a sufficiently strong tendency of the mixture to exhibit liquid+liquid decomposition, that is for sufficiently large values of Λ . Again the three coexistence surfaces connect along the triple line for a certain temperature range. However, now the critical lines bounding the coexistence surfaces between gas, on one hand, and both demixed A-rich and B-rich liquid, on the other hand, may approach the critical line between demixed A- and B-rich liquids from below. Since physically sensible phase diagrams must not have any holes, the only way to fully connect the three coexistence surfaces is to have the triple line ending at a TCP rather than a CEP. This situation is illustrated in Fig. 6. In fact, the existence of this TCP is a direct consequence of the symmetry between A-rich and B-rich liquids, that is $T_c^A=T_c^B$, because $\epsilon_{AA}=\epsilon_{BB}$. The mixtures which exhibit such a TCP are on the vertical thick solid line at $\zeta=0$ in Fig. 1 at which $\epsilon_{AA}=\epsilon_{BB}$.

This logic also suggests that there might be a special situation at which $T_c^A=T_c^B=T_c^L$, such that each of the critical lines is approached by the two other ones from below. This situation is, in fact, realized in Fig. 5, where we see that again the critical lines merge tangentially with a triple line, which gives rise to three rather than just a single TCP. These three triple lines now give rise to a fourth phase, namely that of the mixed liquid. The three triple lines branch off a triple line between gas, A-rich, and B-rich demixed liquid phases at the quadruple point (see Fig. 5). However, this situation may be rather arcane with respect to a realization in any experimental systems, but once again emphasizes the important role of geometry in the context of complex phase diagrams. At least it may be exceedingly difficult to prepare an experimental system represented by an isolated point in thermodynamic state space.

Even though these symmetry arguments seem plausible for symmetric mixtures (i.e., because of $\epsilon_{AA}=\epsilon_{BB}$), it seems quite surprising at first that TCPs do arise even in *asymmetric* mixtures, because our above argument based upon the mutual dependence of criticality between gas and both A- and B-rich liquids seems entirely inapplicable as far as asymmetric mixtures are concerned. The obvious reason is that because of $\zeta \neq 0$ ($\epsilon_{AA} \neq \epsilon_{BB}$), the variation of the critical lines ending at C_A and C_B is no longer symmetric with respect to the plane $\Delta\mu=0$.

The key to understanding that we might still observe TCPs despite the asymmetry of the mixture is to realize first that the role of the critical points C_A , C_B , and C_L may be inverted in the sense that one may now generate a situation in which $T_c^B=T_c^L < T_c^A$ (i.e., $\epsilon_{BB}=\epsilon_L < \epsilon_{AA}$) as shown in Fig. 9. In fact, the phase diagram presented in that figure may be perceived as being geometrically equivalent to the one shown in Fig. 6 for a *symmetric* mixture but rotated by an angle of $3\pi/4$ in the μ - $\Delta\mu$ plane with the role of C_A and C_L interchanged with regard to the relative magnitudes of the critical temperatures T_c^A and T_c^L . Hence, the same geometric arguments presented in conjunction with phase diagrams for *symmetric* mixtures applies to *asymmetric* ones as well with the difference that the role of the participating coexistence surfaces has to be changed. To summarize, we observe a TCP due to the symmetry condition $\epsilon_{BB}=\epsilon_L$ in all mixtures represented by the thick solid line for $\zeta > 0$ in Fig. 1. Moreover, mixtures obeying $\epsilon_{AA}=\epsilon_L$ (see the other thick solid line in Fig. 1 for $\zeta < 0$) also exhibit a TCP.

However, the three coexistence surfaces may connect along a triple line ending in a CEP if the tendency of the liquid phase to decompose is large enough. This situation is depicted in Fig. 10, where the enhanced tendency of the mixture to decompose causes C_A , C_B , and C_L to be ordered such that $T_c^A > T_c^L > T_c^B$. Note again that this can be perceived as being geometrically equivalent to the situation shown in Fig. 4 for a *symmetric* mixture with the phase diagram rotated in the μ - $\Delta\mu$ plane by $3\pi/4$.

Hence, we see that whether or not TCPs arise depends crucially on the geometry of the coexistence surfaces between gas and both demixed A- and B-rich liquids and the one describing coexistence between the latter two phases. The reader should note that the relation between symmetry properties of the (complete) phase diagram and existence of TCPs established in this work is far more general than the one linking TCPs to the symmetry of the intermolecular in-

teractions [28]. The former, in conjunction with the physical requirement that coexistence surfaces must be fully connected, poses the necessary geometrical conditions that determine whether or not TCPs may exist in binary mixtures. Thus, we conclude that only on the basis of a calculation of *complete* phase diagrams as in this work, the relation between TCPs and other geometrical features such as triple and critical lines can be fully understood.

The necessity to calculate *complete* phase diagrams rather than special cuts through those becomes particularly apparent if one considers the cut along the line $\Delta\mu=0$ previously investigated in the literature for the special case of symmetric binary mixtures [17,30]. If one focuses on this cut, one inevitably misses two of the three TCPs shown in Fig. 5 (see Fig. 2(c) of Ref. [17] and Figs. 1(b) and 1(c) of Ref. [30]). Moreover, the role of azeotropy in the *complete* phase diagrams was completely missed in these earlier studies, which causes the classification scheme employed by Wilding *et al.* [17] and later also adopted by us [30] to be inadequate and inconsistent with the one proposed by van Konynenburg and Scott [4].

In closing, we emphasize that the special class of symmetric binary mixtures at $\Delta\mu=0$ is interesting because of its relation to a number of other important model fluids. For example, pure ferroelectric liquids without external fields can be mapped onto the symmetric binary mixtures at $\Delta\mu=0$. Here it turns out that ordered phases in the ferroelectric liquid (characterized by either “spin up” or “spin down”) correspond to demixed A- or B-rich liquid phases, whereas isotropic phases in ferroelectric liquids correspond to mixed phases in the present model mixtures [35–43]. The same correspondence applies to liquid ^3He - ^4He mixtures, where the superfluid states of ^4He correspond to demixed liquid states in our model; likewise, the ^3He - ^4He coexistence may be interpreted as coexistence between gas and demixed liquid in our model. In fact, as we note in passing the shape of the peak in the heat capacity of pure ^4He at the superfluid transition gave rise to the term “ λ line” usually associated with the critical line in symmetric binary mixtures of type III-HA [44].

ACKNOWLEDGMENTS

This work was supported by the Deutsche Forschungsgemeinschaft in the framework of the Sonderforschungsbereich 448 “Mesoskopisch strukturierte Verbundsysteme.” The authors thank Gabriel Range for fruitful discussions.

-
- [1] J. S. Rowlinson and F. L. Swinton, *Liquids and Liquid Mixtures*, Butterworths Monographs in Chemistry, 3rd ed. (Butterworths, London, 1982).
- [2] G. R. Gray, H. C. H. Darley, and W. F. Rogers, *Composition and Properties of Oil Well Drilling Fluids*, 4th ed. (Gulf, Houston, 1980).
- [3] P. K. Chabibullaev and A. A. Saidov, *Phase Separation in Soft Matter Physics*, Springer Series in Solid-State Sciences Vol.

138 (Springer, Berlin, 2003).

- [4] P. H. van Konynenburg and R. L. Scott, *Philos. Trans. R. Soc. London, Ser. A* **298**, 495 (1980).
- [5] D. Furman, S. Dattagupta, and R. B. Griffiths, *Phys. Rev. B* **15**, 441 (1977).
- [6] D. Furman and R. B. Griffiths, *Phys. Rev. A* **17**, 1139 (1978).
- [7] L. Z. Boshkov, *Dokl. Akad. Nauk SSSR* **294**, 901 (1987).
- [8] P. H. E. Meijer, *J. Stat. Phys.* **53**, 543 (1988).

- [9] M. Keskin, M. Gencaslan, and P. H. E. Meijer, *J. Stat. Phys.* **66**, 885 (1992).
- [10] U. K. Deiters and I. L. Pegg, *J. Chem. Phys.* **90**, 6632 (1989).
- [11] T. Kraska and U. K. Deiters, *J. Chem. Phys.* **96**, 539 (1992).
- [12] A. van Pelt and T. W. de Loos, *J. Chem. Phys.* **97**, 1271 (1992).
- [13] G. Jackson, J. S. Rowlinson, and C. A. Leng, *J. Chem. Soc., Faraday Trans. 1* **82**, 3461 (1986).
- [14] X. S. Chen and F. Forstmann, *J. Chem. Phys.* **97**, 3696 (1992).
- [15] N. B. Wilding and P. Nielaba, *Phys. Rev. E* **53**, 926 (1996).
- [16] N. B. Wilding, *Phys. Rev. E* **55**, 6624 (1997).
- [17] N. B. Wilding, F. Schmid, and P. Nielaba, *Phys. Rev. E* **58**, 2201 (1998).
- [18] N. B. Wilding, *Phys. Rev. E* **67**, 052503 (2003).
- [19] I. Nezbeda, J. Kolafa, and W. R. Smith, *J. Chem. Soc., Faraday Trans.* **93**, 3073 (1997).
- [20] J. Kolafa, I. Nezbeda, J. Pavlíček, and W. R. Smith, *Fluid Phase Equilib.* **146**, 103 (1998).
- [21] L. V. Yelash and T. Kraska, *Ber. Bunsenges. Phys. Chem.* **102**, 213 (1998).
- [22] D. A. Lavis and G. M. Bell, *Statistical Mechanics of Lattice Systems: Closed-Form and Exact Solutions*, 2nd ed. (Springer, Berlin, 1999), Vol. 1.
- [23] J.-L. Wang, G.-W. Wu, and R. J. Sadus, *Mol. Phys.* **98**, 715 (2001).
- [24] M. H. Lamm and C. K. Hall, *AIChE J.* **47**, 1664 (2001).
- [25] G. Kahl, E. Schöll-Paschinger, and A. Lang, *Chem. Monthly* **132**, 1413 (2001).
- [26] O. Antonevych, F. Forstmann, and E. Diaz-Herrera, *Phys. Rev. E* **65**, 061504 (2002).
- [27] A. Mejía, J. C. Pàmies, D. Duque, H. Segura, and L. F. Vega, *J. Chem. Phys.* **123**, 034505 (2005).
- [28] D. Pini, M. Tau, A. Parola, and L. Reatto, *Phys. Rev. E* **67**, 046116 (2003).
- [29] A. S. Wightman, in *Convexity in the Theory of Lattice Gases*, edited by R. B. Israel, Princeton Series in Physics (Princeton University Press, Princeton, NJ, 1979), pp. ix–lxxxv.
- [30] D. Woywod and M. Schoen, *Phys. Rev. E* **67**, 026122 (2003).
- [31] J. R. Silbermann, D. Woywod, and M. Schoen, *Phys. Rev. E* **69**, 031606 (2004).
- [32] P. W. Atkins and J. d. Paula, *Atkins Physical Chemistry*, 7th ed. (Oxford University Press, Oxford, 2002).
- [33] D. Woywod, PhD dissertation, Fakultät II, Technische Universität, 2004 (unpublished); http://edocs.tu-berlin.de/diss/2004/woywod_dirk.htm
- [34] R. J. Baxter, *Exactly Solved Models in Statistical Mechanics*, 3rd ed. (Academic, San Diego, CA, 1990), Vol. 1.
- [35] P. C. Hemmer and D. Imbro, *Phys. Rev. A* **16**, 380 (1977).
- [36] W. Fenz and R. Folk, *Phys. Rev. E* **67**, 021507 (2003).
- [37] B. Groh and S. Dietrich, *Phys. Rev. E* **50**, 3814 (1994).
- [38] H. Zhang and M. Widom, *Phys. Rev. E* **49**, R3591 (1994).
- [39] E. Lomba, J.-J. Weis, N. G. Almarza, F. Bresme, and G. Stell, *Phys. Rev. E* **49**, 5169 (1994).
- [40] J. M. Tavares, M. M. Telo da Gama, P. I. C. Teixeira, J.-J. Weis, and M. J. P. Nijmeijer, *Phys. Rev. E* **52**, 1915 (1995).
- [41] J.-J. Weis, M. J. P. Nijmeijer, J. M. Tavares, and M. M. Telo da Gama, *Phys. Rev. E* **55**, 436 (1997).
- [42] A. Oukouiss and M. Baus, *Phys. Rev. E* **55**, 7242 (1997).
- [43] G. M. Range and S. H. L. Klapp, *Phys. Rev. E* **69**, 041201 (2004).
- [44] M. Chan, N. Mulders, and J. Reppy, *Phys. Today* **49**(8), 30 (1996).